ISSN 1392 - 1207. MECHANIKA. 2014 Volume 20(1): 24-34

Evaluation of heat transfer on a backward acting grate

Bernhard Peters*, Algis Džiugys**
**Université du Luxembourg, Campus Kirchberg, 6, rue Coudenhove-Kalergi, L-1359 Luxembourg, Luxembourg, E-mail: bernhard.peters@uni.lu*
***Lithuanian Energy Institute Breslaujos g. 3, LT-44403 Kaunas, Lithuania, E-mail: dziugys@mail.lei.lt*

crossref http://dx.doi.org/10.5755/j01.mech.20.1.3775

1. Introduction

Thermal conversion of solid fuel is a complex interaction of fluid flow, heat and mass transfer within both moving and fixed beds of fuel particles. An accurate description of fluid flow through packed beds and its mass and heat transfer is important to the design of packed bed reactors. The solution of this problem requires an extensive knowledge of heat transfer and mass transfer characteristics within the bed. Although heat and mass transfer in packed beds and to the fluid are widely applied in various domains, it is largely based on empirical correlations. The latter often describe heat transfer insufficiently, and therefore, require more intensive investigations.

Experiments with a high resolution tend to be very expensive, while the costs of numerical approaches even including a large degree of details decrease. Thus, numerical models including computational fluid dynamics (CFD) have proven to be a reliable tool to evaluate the interaction of fluid and packed beds. It allows extracting a deeper knowledge of heat and mass transfer within complex geometries and leads to better understanding of the phenomena involved without a continuous phase being required. Among them are the different modes of heat transfer namely conduction, convection and radiation.

1.1. Modes of heat transfer

1.1.1. Conductive heat transfer

Conductive heat transfer in granular systems may be described simply by conduction between the particles in contact and no continuous phase is required. Smirnov et al. [1, 2] investigated experimentally radial heat transfer between a packed bed and walls. The flow of heat in a rotating tumbler containing granular material was studied by Figueroa et al. [3] dependent on the cross-sectional shape of the tumbler, degree of filling and rotational speed. The approach of thermal particle dynamics (TPD) was employed, which assumes that the temperature gradients propagate only within the nearest neighbours of any given particle during a single time step. The Pèclet number for granular systems was defined as the ratio of the mixing rate and the rate of thermal diffusion. In order to quantify the impact of mixing on the overall rate of heat transfer, the "apparent heat transfer coefficient" was applied, relating the wall temperature and the average temperature in the granular bed. It has been shown that increasing mixing rates might decrease the rate of heating of the granular bed, because at higher mixing rates, the contact times between the particles are reduced.

1.1.2. Convective heat transfer

Convective heat transfer is distinguished in free and forced convection, whereby forced convection in particular in engineering applications has a higher importance.

Free convection. Laguerre et al. [4] investigated into two modelling approaches of transient heat transfer due to free convection in a packed bed of spheres. The first approach employed computational fluid dynamics software, which directly solves the Navier–Stokes equations and the local energy equations in the fluid and solid phase. Additionally, it included radiation between the solid surfaces. In the second approach, methods developed for porous media and packed beds were applied. The heat transfer model, based on a dispersed particle approach, takes into account air-particle convection, conduction and radiation between particles. One-dimensional conduction to describe the temperature distribution inside particles was used. The numerical results obtained including particle temperature using the two approaches were in good agreement with the experimental values of air for a free convection configuration.

Forced convection. Radial and axial heat transfer between walls and a packed bed of spheres (diameter $d = 3.8$ cm) with an air flow of rather low velocity was studied by Laguerre et al. [5]. Their approach distinguished into fluid and solid phase temperatures to characterize the heat transfer between both wall and air and between wall and adjacent particles. It was found that the air velocity and the arrangement of particles along the wall are of great influence to the convective heat transfer in the voids near the wall and particles. However, the effect of temperature difference between the wall and the air is negligible. Swailes and Potts [6] developed and analysed models for transient forced convection of a heated gas through granular porous media of low thermal conductivity. Venugopal et al. [7] experimentally investigated the potential of a simple and inexpensive porous inserts developed specifically for augmenting heat transfer from the heated wall of a vertical duct under forced flow conditions. The characteristic features of the porous medium model on the hydrodynamic and heat transfer behaviour have also been investigated. They developed of a new correlation for the Nusselt number that does not require any information from hydrodynamic studies. Over the range of parameters considered, the largest increase in the average Nusselt number of 4.52 times that for clear flow is observed with a porous material of porosity of 0.85.

1.1.3. Radiative heat transfer

The design of efficient burners, furnaces and

other systems based on combustion requires accurate prediction of heat transfer rates in these systems. Conductive and convective heat transfer rates are generally proportional to the temperature difference, while radiative heat transfer is proportional to the fourth power of the temperature. Therefore, an accurate evaluation of thermal radiation is very important in combustion applications, where the total heat transfer may consist mainly of thermal radiation. It may amount of up to 40% in fluidized bed combustion and 90% in large-scale coal combustion chambers.

Hence, prediction of the heat transfer process in a typical high-temperature energy conversion device such as an internal combustion engine includes apart from equations for momentum, turbulence and mass one general equation for energy conservation incorporating all three modes of heat transfer. It comprises convection, conduction and radiation where the radiative heat transfer part represents an integro-differential equation that deals with seven independent variables:

- time and three space coordinates;
- two angles describing the direction of travelling photons;
- frequency of radiation,

while conduction and convection involve a maximum of four independent variables namely time and three space coordinates. A solution of the integro-differential equation for radiation in general is extremely complicated and may only be resolved by efficient and cost-effective models that could predict radiative heat transfer rates with required accuracy. Furthermore, despite the fact that radiation remains the dominant mode of heat transfer conduction and convection also have to be considered to evaluate the total heat transfer rate. Therefore the variation in radiative heat transfer in a packed bed as a function of the solid conductivity is of critical importance and deserves considerable attention.

1.2. Mathematical approaches and models

Flow of a fluid through a packed bed may be treated by two approaches: in a direct simulation approach, the fluid flow is resolved through the void space between particles. A more general approach approximates fluid flow through the packed bed as flow through porous media. Both approaches are classified coarsely in the so-called two-phase (two-equations) and single-phase (homogeneous one-equation) models.

1.2.1. One-phase (homogeneous) models

This class of models rely on an averaging process over the solid and gaseous phase and therefore may be most easily treated by a CFD approach expanding into several dimensions. An additional parameter that influences the heat transfer in a packed bed is the ratio of thermal capacity of the packed bed and the fluid flow in the void space. If the thermal capacity of the fluid is high compared to the packed bed, rather homogeneous temperature profiles develop, as shown by measurements of Thomèo and Grace [8].

Fanaei and Vaziri [9] predicted heat transfer in a bioreactor by a simple model, that excluded mixing as it would influence negatively the biomaterial in the reactor. A "lumped" model neglected spatial variations of temperature, whereas a distributed model includes the axial dependence. Both models were employed to predict the growth of biomass in a reactor.

Moreira et al. [10] investigated into the heat transfer in packed beds by five pseudo-homogeneous models. The models do not distinguish in different phase due to the difficulty of measuring temperatures of fluids and particles individually. Pseudo-homogeneous models are described by the following differential conservation equation:

$$Gc_{pg} + Lc_{pl}\frac{\partial T}{\partial z} = k_r\left[\frac{1}{r}\frac{\partial}{\partial r}\left(r\frac{\partial T}{\partial r}\right)\right] + k_a\frac{d^2T}{\partial z^2}, \qquad (1)$$

where G, L, c_{pg}, c_{pl}, k_r, k_a are the superficial gas and liquid flow rates, gas and liquid heat capacities, effective radial and axial thermal conductivities, respectively. Different models differ in boundary conditions, inclusion or exclusion of axial thermal conductivity and treatment of the wall heat transfer coefficient. The experimental set-up consisted of a cylindrical column (Ø5 cm, length 80 cm), filled with glass spheres (sizes between 1.9 and 4.4 mm), through which air and water streamed. A comparison between measurements and predictions yielded good agreement.

Many studies rely on the radial effective heat conductivity λ_{eff} and the heat transfer coefficient at the wall α_w in packed beds to describe heat transfer. Such an approach requires thermal equilibrium between the two phases of a packed bed and is referred to as the one-equation model. Regin et al. [11] applied a one-equation model to predict the dynamic behaviour during charging and discharging of a packed bed latent heat thermal energy storage system. The packed bed consisted of spherical capsules filled with paraffin wax. They found that a solidification period is longer than a melting period due to a reduced heat transfer during solidification. Furthermore, charging and discharging rates are significantly higher for the capsule of smaller radius compared those of larger radius.

In order to apply CFD-derived methods in particular differential conservation equations in space and time to packed beds, relevant variables such as temperature, velocity or specie concentrations are averaged over the heterogeneous structure of a packed as employed by de Souza et al. [12].

Polesek-Karczewska [13] measured the temperature distribution of a heated packed bed of different materials. Furthermore, they correlated the experimental data with theoretical and numerical approaches for a homogeneous phase model. They concluded that value of conductivity determined for non-homogeneous materials appears to be higher than the effective thermal conductivity determined by widely used formulae from the literature under steady state conditions.

Smirnov et al. [1, 2] carried out a study for radial heat transfer in tubular packed beds consisting of cylindrical beds formed of spheres, cylinders and Rashig rings under steady state conditions. They aimed at determining heat transfer parameters for the standard dispersion model (SDM). As a conclusion, the radial thermal conductivity for all cylindrical particles with arbitrary number and form of the channels is described by one formula with constant parameters.

1.2.2. Two-phase (heterogeneous) models

The homogeneous phase models of the previous

section rely on thermal equilibrium between the phases considered. However, without thermal equilibrium the thermal transport in each phase and the transfer between them has to be considered.

MacPhee and Dincer [14] investigated into the thermal energy storage system of ice capsules embedded in a liquid. During the charging process heat is retrieved from the ice capsules to cool the liquid, and thus, causing the ice inside the capsules to melt. Conversely, during discharge a liquid with a temperature below the melting point was in contact with the packed bed of ice capsules so that the ice capsules froze again, and thus, "store the cold". The set of ice capsules is modelled as a continuous porous media, rather than the set of discrete particles.

Direct numerical simulation is increasingly applied to study heat transfer between two phases. Although, it is considered to be the most accurate approach it is very expensive in terms of computer resources and only a small area of the packed bed may be analysed nowadays. Lee et al. [15] predicted the flow in the core of a pebble bed reactor and its heat transfer. They concluded that results depend significantly on the modelling of the inter-pebble region, because the treatment of the contacts among the pebbles with approximated gaps may give inaccurate information about the local flow fields.

In general, bed reactors may be classified into the ordered packed bed reactors and randomly packed reactors. The latter type is easier to implement and use, however, they experience much higher-pressure drop and the overall heat transfer efficiency might be greatly reduced. Structured packing can reduce the pressure drop and improve the heat transfer performance. Simulations of the metal structured packed beds were reported in [16]. Their set-up consisted of a cylindrical arrangement of a number of axially parallel channels, discretised by a finite volume mesh. The flow medium was air treated as an ideal gas. It was found that at low Reynolds number values, the heat transfer capability is mostly determined by the specific surface area, while at high Reynolds number values, the property of solid phase and structure of void space is an important factor.

The effect of packing arrangement and particle shapes on flow and heat transfer inside the pores of different types of structured packed beds was studied numerically in [17]. The set-up consisted of 8 packed cells with symmetric boundary conditions. Spherical, flat ellipsoidal and long ellipsoidal particles were used, which were arranged in simple cubic, body centre cubic and face centre cubic lattices. The fluid flow inside the pores was described by three-dimensional Navier-Stokes and energy equations for steady incompressible flow. For $Re > 300$, the RNG k - ε turbulence model and a scalable wall function were used. The flow in packed beds was considered as flow in a porous media, where the macroscopic hydrodynamics is modelled by an extended Forchheimer-Darcy approximation. It was found that a proper selection of the packing form and the particle shape can reduce significantly the pressure drop in structured packed beds and improve the heat transfer performance.

The flow in an unstructured packing of polydisperse spherical particles with a value of polydispersity deviating by 14 % from the mean diameter was considered in [18]. A dense packing of spheres was generated using DEM, neglecting the friction between particles and between the particles and the walls. Drag coefficients and Nusselt numbers were calculated applying CFD for a single sphere and for two spheres located close to each other. These results were transformed to a packed bed in a column. In order to reduce computational efforts two domains as a pie-shaped including the near-wall region and a region from the bulk far from the walls were extracted from the packed bed. The number of particles in these domains were 620 and 440, respectively. The hydrodynamics and heat transfer equations were solved in the range of Reynolds and Schmidt numbers of $1 < Re < 100$ and $300 < Sc < 1000$. The results indicated that contraction of particles applied to the packing in order to enable finite-volume meshing leads to underestimation of the transverse dispersion.

Papadikis et al. [19] studied the heat transfer conditions dependent on the size of biomass particles exposed to a fluidised bed of sand and undergoing pyrolysis. The size of the sand particles was 400 μm, while two size fractions (350 μm) and larger (550 μm) of biomass particles were used. Conductive heat transfer was considered for larger biomass particles and was neglected for smaller biomass particles. The gas phase as a nitrogen gas was described by the Eulerian approach while the solid phase model was based on the radial distribution function and the granular temperature. Both phases were coupled through the particle drag force in the continuum and heat transfer along the particle radius by solving the heat diffusion equation for an isotropic particle. It has been found that different heat transfer mechanisms are involved for particles of different sizes, resulting in different heat transfer coefficients. The temperature gradients inside the particles could be neglected due to small Biot numbers. According to the study, smaller particles yielded better results for fast pyrolysis applications, because they are better entrained in the bed during degradation. Smaller size reduced the effect of secondary reactions resulting in higher yields of bio-fuels.

An extensive review of a problems and models of fluid flow, heat and mass transfer in porous media may be found in [5-7, 20, 21].

2. Description of the discrete particle method

An increasing environmental awareness demands reductions in energy consumption by better efficiency and a sustainable treatment of energy sources. In order to comply with a sustainable approach, a deeper knowledge of energy conversion or energy producing processes has to be gained which is addressed by the discrete particle method (DPM). Relevant areas of application are furnaces for wood combustion, blast furnaces for steel production, fluidised beds, cement industry or predictions of emissions concerning air quality. Each of these applications represents complex processes involving various aspects of thermodynamics, fluid dynamics, chemistry and physics. Hence, the discrete particle method is an advanced multi-physics and numerical simulation tool which deals with both motion and chemical conversion of particulate material in conjunction with computational fluid dynamics (CFD) [21]. However, predictions of solely motion or conversion in a de-coupled mode are also applicable.

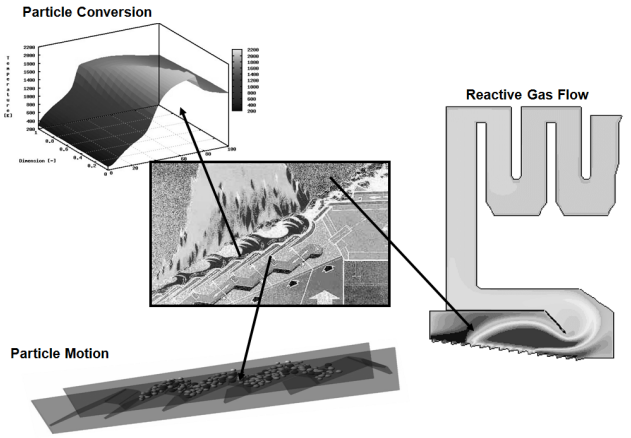

Fig. 1 Approach of the DPM

Contrary to the continuum approach, the DPM considers a solid fuel particle as an individual entity with above-mentioned conversion and motion attached to it. Hence, the sum of all particle processes represents the entire process like of a moving and fixed bed and may be summarised with the following formula:

$$Entire\ Process = \sum Particle\ Processes + CFD\ .$$

This approach includes three major areas as depicted in the Fig. 1:

- Thermal conversion of particles due to chemistry (conversion module);
- Motion and rotation of particles due to contact and external forces (motion module);
- Reacting flow in the void space between the particles in conjunction with heat and mass transfer between the particle's surface and the gas CFD.

The above-mentioned aspects are dealt with individually by the motion and conversion modules. Conversion encompasses a large variety of chemo-physical processes such as drying, pyrolysis, devolatilization, gasification or combustion. These particle specific processes are described by a set of one-dimensional and transient differential conservation equations including interactions such as heat transfer between neighbouring particles. The solution of these equations yields the distribution of temperature and species e.g. carbon-dioxide or alkali salts inside a particle versus time.

With the following assumptions:

- one-dimensional and transient behaviour;
- particle geometry represented by slab, cylinder or sphere;
- thermal equilibrium between gaseous, liquid and solid phases inside the particle,

the differential conservation equation for energy describes the thermal behaviour of a particle:

$$\frac{\partial\left(\rho c_p T\right)}{\partial t} = \frac{1}{r^n}\frac{\partial}{\partial r}\left(r^n \lambda_{\text{eff}} \frac{\partial T}{\partial r}\right) + \sum_{k=1}^{l} \dot{\omega}_k H_k\,, \qquad (2)$$

where n defines the geometry of a cylinder ($n = 1$) or sphere ($n = 2$), ρ is the density, c_p is the heat capacity at constant pressure, T - temperature. The source term on the right-hand side of (1) represents heat release or consumption due to chemical reactions $k = 1,..., l$, with reaction rate $\dot{\omega}$ and reaction enthalpy H_k. According to [22], the locally varying heat conductivity, λ_{eff} is evaluated as:

$$\lambda_{\text{eff}} = \varepsilon_P \lambda_g + \eta\lambda_{\text{wood}} + (1-\eta)\lambda_c + \lambda_{\text{rad}}\,, \qquad (3)$$

which takes into account heat transfer by conduction in the gas, solid, char and radiation in the pore, respectively. ε_P defines porosity. The source term on the right hand side represents heat release or consumption due to chemical reactions.

Motion of particles in a rotary kiln or on a moving grate is derived from the discrete element method (DEM) and describes the trajectory of each particle. By describing the degrees of freedom for each particle its motion is entirely determined. Newton's Second Law for conservation of linear and angular momentum describe position and orientation of a particle i as follows:

$$m_i \frac{d^2\vec{r}_i}{dt^2} = \sum_{i=1}^{N} \vec{F}_{ij}(\vec{r}_j, \vec{v}_j, \vec{\varphi}_j, \vec{\omega}_j) + \vec{F}_{\text{extern}}\,; \qquad (4)$$

$$\bar{I}_i \frac{d^2\vec{\phi}_i}{dt^2} = \sum_{i=1}^{N} \vec{M}_{ij}(\vec{r}_j, \vec{v}_j, \vec{\phi}_j, \vec{\omega}_j) + \vec{M}_{\text{extern}}\,, \qquad (5)$$

where $\vec{F}_{ij}(\vec{r}_j, \vec{v}_j, \vec{\phi}_j, \vec{\omega}_j)$ and $\vec{M}_{ij}(\vec{r}_j, \vec{v}_j, \vec{\phi}_j, \vec{\omega}_j)$ are the forces and torquues acting on a particle i of mass m_i and tensotial moment of inertia $\bar{I}_i$. Both forces and torques depend on position $\vec{r}_j$, velocity $\vec{v}_j$, orientation $\vec{\phi}_j$, and angular velocity $\vec{\omega}_j$ of neighbour particles j that undergo impact with particle i. The contact forces comprise all forces as a result from material contacts between a particle and its neighbours. Forces may include external forces due to moving grate bars, fluid forces and contact forces between the particles in contact with a bounding wall. This results in a system of coupled non-linear differential equations which usually cannot be solved analytically.

Treatment of a flow of reacting gases in the voids is dealt with by well-established CFD-tools.

Initial and boundary conditions. According to [23] the Nusselt number Nu for heat transfer of a sphere evaluates as:

$$Nu = f\,Nu_{m,sphere}\,, \qquad (6)$$

for a packed bed with f and $Nu_{m,sphere}$ being an empirical correlation $f = 1 + 1.5\,(1 - \varepsilon)$ and the mean Nusselt number for a spherical geometry, respectively. Under laminar conditions the latter is defined by:

$$Nu_{m,\text{sphere}} = 2.0 + 0.664 Re^{1/2} Pr^{1/3}\,, \qquad (7)$$

where Re and Pr denote the Reynolds and Prandlt number ($Pr \sim 0.68$ [24]), respectively.

Hence, the following boundary condition for heat transfer of a particle is applied:

$$-\lambda_{\text{eff}} \frac{\partial T}{\partial r}|_R = \alpha(T_R - T_\infty) + \dot{q}_{\text{cond}} + \dot{q}_{\text{rad}}\,, \qquad (8)$$

where T_∞, $c_{i,\infty}$, α and β denote ambient gas temperature, concentration of specie i, heat and mass transfer coefficients, respectively.

The DPM uses object-oriented techniques that support objects representing three-dimensional particles of various shapes, size and material properties. This makes DPM a highly versatile tool dealing with a large variety of different industrial applications of particulate materials. For a detailed description the reader is referred to [25].

3. Results and discussion

As mentioned in the previous section the DPM is employed to predict both motion and heat-up of individual particles of a moving bed on a backward acting grate. Motion of the particles was predicted by the traditional approach of the DEM, while energy conservation was employed to predict the temporal and spatial distribution of temperature for each particle. It takes into account conduction and radiation between particles and convective heat transfer between the particles and the surrounding flow field. Particles were approximated by spheres and the material was represented by fir wood. The packed bed was exposed to a constant specific radiative flux from above of $\dot{q}''$ = 30 kW/m^2. In order to exclude the effect of a locally varying convective heat transfer of the gas phase in the voids of a packed bed gas temperature as ambient temperature of T_{amb} = 300 K for the particles and heat transfer coefficient α = 20 W/m^2 K were set constant.

Table 1

Thermodynamic properties of fir wood

Property	Fir wood	Ash
Density ρ	310 kg/m^3	1000 kg/m^3
Specific heat c_p	1733 J/kg·K	1400 J/kg·K
Conductivity λ	0.2 W/m·K	0.93 W/m·K
Porosity ε	0.6	0.3
Pore diameter d_p	50 µm	50 µm
Tortuosity τ	1	1

Table 2

Mechanical properties of fir wood

Property	Fir wood
Radius r	12.5 mm
Young's modulus E	0.01 MPa
Shear modulus G	0.003 MPa
Poisson ratio σ	0.2
Dynamic friction μ	0.8
Normal dissipation v_n	200 1/s
Tangential dissipation v_t	200 1/s

A particle composition amounts to 97% fir wood and 3% ash of which the thermodynamic and mechanical properties are listed in the following Tables 1 and 2.

In order to reduce simulation time, the simulation space represented a particular section of the grate and periodic boundary conditions were employed at the entry and exit of the grate. Hence, particles that left the grate at the exit, were periodically introduced at the entry of the grate, and thus, reflect a sequence of grate sections as shown in Fig. 2.

The grate is inclined by an angle of α_G = 24°, whereas the bar angle is α_B = 40°. Every second grate bar moves periodically forward and backward and the bars between the moving bars were kept at rest. This motion scheme represents the operation mode of a backward acting grate and causes particles to move over the grate through the combustion chamber. Since amplitude and period of moving grate bars effects the residence time of the particles to a large extent [26], these parameters were subject to variation, and its influence on the heat-up was investigated. This included both prediction of the thermal behaviour of each particle on the grate and its subsequent statistical analysis of the moving bed. The former is exemplified for a single particle in Fig. 3 that depicts the evolution of the spatial distribution of temperature over a period of 1000 s.

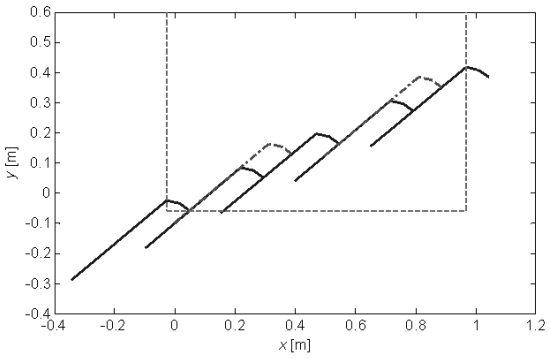

Fig. 2 Geometry of a backward acting grate

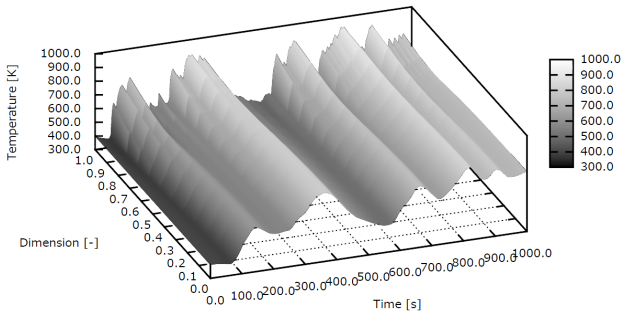

Fig. 3 Temperature distribution of an individual particle on a backward acting grate versus time and space

The particle's inital temperature was set to T = 400 K, so that particles within the packed bed and not subject to surface radiation loose energy to the primary air that causes the particle temperature to decrease. After a period of ~100 s the temperature increases sharply, because the particle is moved to the surface of the packed bed, and therefore, is exposed to radiation. The particle resides for some period on the surface of the moving bed, before it leaves this position and enters the interior of the moving bed due to bar motion. Hence, the particle is shielded by newly evolving surface particles, and therefore, does not receive a further radiation flux. Instead heat transfer occurs to neighbouring particles and primary air that reduces the particle temperature. At a later stage the particle is moved to the bed surface again and exposed to radiation and the cycle of heating and cooling down repeats itself irregularly during the total residence time on the grate.

The temperature distribution of all particles at a time of t = 1000 s is shown in Fig. 4 for an amplitude of A_B = 0.124 m and a periodicity of T_B = 20 s of bar motion and Fig. 5 depicts similarly for an amplitude of A_B = 0.062 m and a periodicity of T_B = 100 s, i.e., a slower bar motion than in Fig. 4.

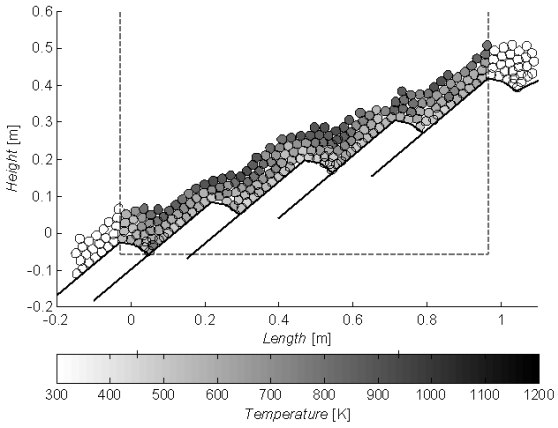

Fig. 4 Temperature distribution of particles on a backward acting grate at a time of $t = 1000$ s subject to a bar amplitude of $A_B = 0.124$ m and a periodicity of $T_B = 20$ s

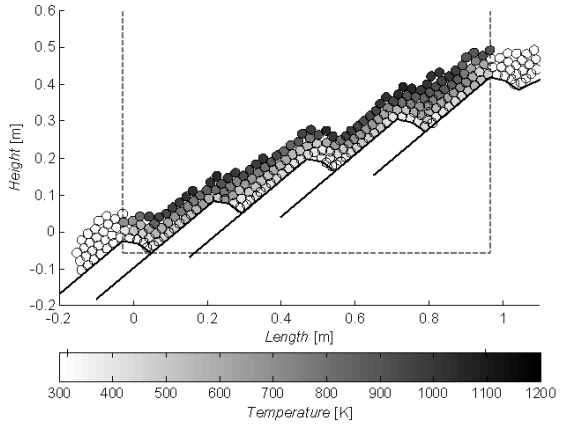

Fig. 5 Temperature distribution of particles on a backward acting grate at a time of $t = 1000$ s subject to a bar amplitude of $A_B = 0.062$ m and a periodicity of $T_B = 100$ s

It becomes apparent that the temperature distribution of particle on a grate with higher bar velocities as shown in Fig. 4 is much more homogeneous than for a lower bar velocity in Fig. 5. Obviously, higher bar velocities cause a better mixing between particles, so that thermal energy is more homogeneously distributed with the moving bed. Moving beds represent a system with complex dynamics dependent on bar velocity, so that particles change both their neighbours and coordination number. This, leads to a varying amounts of heat transferred between particles. Thus, particles are almost randomly exposed to surface radiation for a limited period.

3.1. Statistical analysis of temperature distribution of a moving bed

The influence of bar motion expressed by varying amplitude and periods of the moving bars of a backward acting grate were subject to investigation. Amplitudes of $A_B = 0.062$, 0.124, 0.186 m were combined with periods of $T_B = 10$, 20, 40, 60, 80, 100 s, so that a total number of 18 different cases were predicted (Table 3). The selected amplitudes correspond roughly to a half and a quarter of the total bar length. These combinations correspond to the following mean bar velocities evaluated as $v_B = 2A_B / T_B$.

Table 3

Bar velocities

Amplitude, m	Periodicity, s	Bar velocity, m/s
0.062	10	0.0124
0.062	20	0.0062
0.062	40	0.0031
0.062	60	0.00207
0.062	80	0.00155
0.062	100	0.00124
0.124	10	0.0248
0.124	20	0.0124
0.124	40	0.0062
0.124	60	0.00413
0.124	80	0.0031
0.124	100	0.00248
0.186	10	0.0372
0.186	20	0.0186
0.186	40	0.0093
0.186	60	0.0062
0.186	80	0.00465
0.186	100	0.00372

For each case statistical moments such as minimum, maximum, mean temperature and its deviation versus time of a moving bed were evaluated and are shown in Figs. 6 to 17 sorted by amplitudes and periodicity appearing as a parameter. A uniform line style represents a single amplitude, whereas the colour stands for different periods. Figs. 6-8 depicts the evolution of minimum particle temperature in a moving bed.

The minimum particle temperature varies between 320 and 520 K depending on the parameters set. In general, a higher bar velocity favours an increasing of the minimum temperature. A higher bar velocity causes an increased mixing of particles, and thus, a improved heat transfer. Thus, particles experience more frequently heat transfer in addition to cooling conditions of primary air. At lower bar velocities a reduced mixing forces particles close to the bars to reside there, and thus, exposes them mainly to convective heat transfer with primary air. Therefore, these particles approach a temperature close to the primary air temperature leading to reduced minimum temperatures.

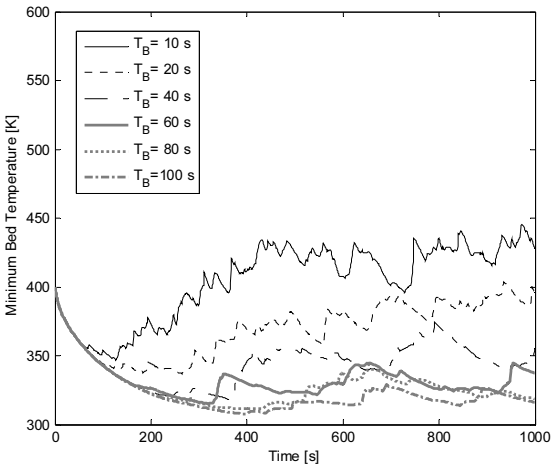

Fig. 6 Evolution of particles' minimum temperature on a backward acting grate dependent on and period bar amplitude $A_B = 0.062$ m

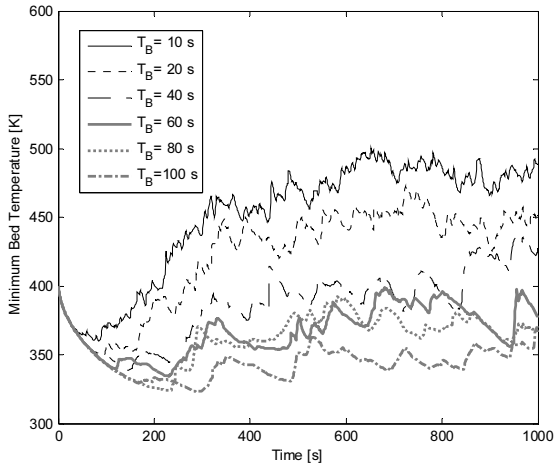

Fig. 7 Evolution of particles' minimum temperature on a backward acting grate dependent on and period bar amplitude A_B = 0.124 m

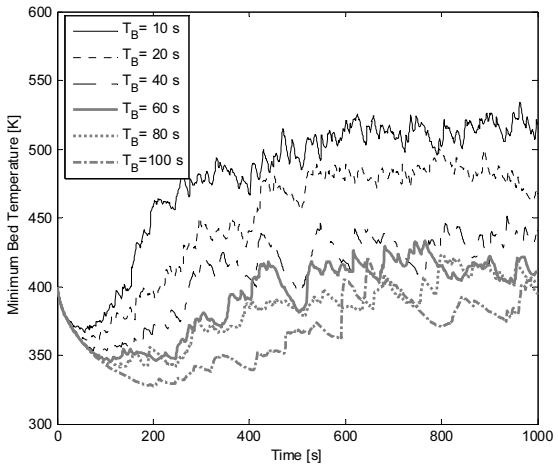

Fig. 8 Evolution of particles' minimum temperature on a backward acting grate dependent on and period bar amplitude A_B = 0.186 m

An inverse characteristic becomes apparent for the evolution of maximum temperature depicted in Figs. 9-11, that decreases with increasing bar velocity. The same mechanism of better mixing for higher bar velocities homogenizes the temperature field because heat is redistributed at a higher rate.

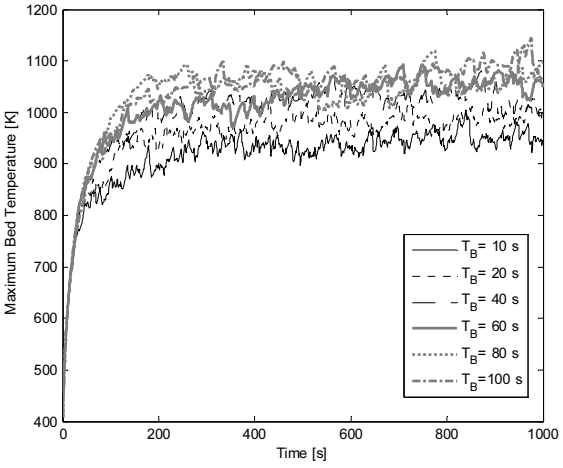

Fig. 9 Evolution of particles' maximum temperature on a backward acting grate dependent on bar period and amplitude A_B = 0.062 m

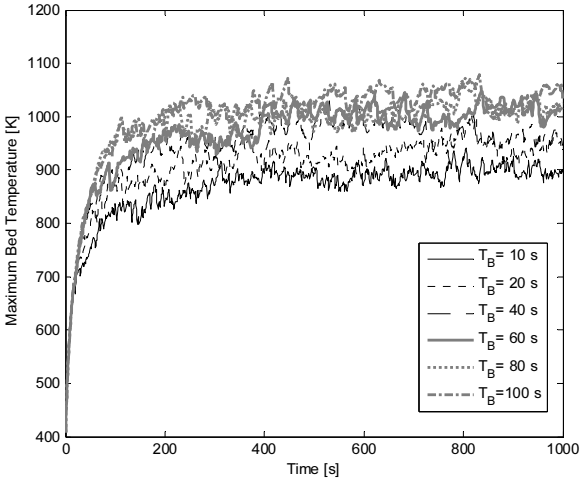

Fig. 10 Evolution of particles' maximum temperature on a backward acting grate dependent on bar period and amplitude A_B = 0.124 m

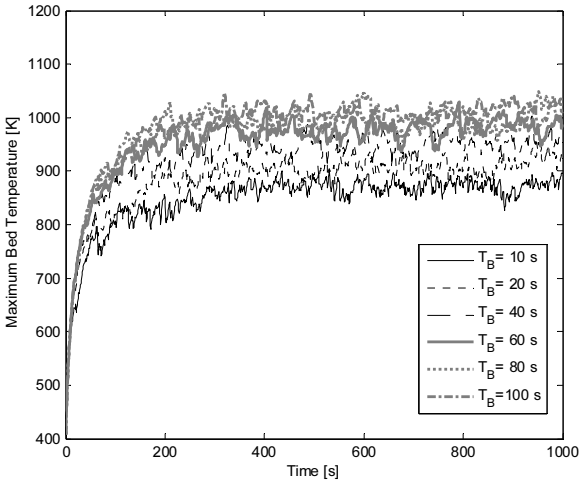

Fig. 11 Evolution of particles' maximum temperature on a backward acting grate dependent on bar period and amplitude A_B = 0.186 m

Figs. 12-14 shows the evolution of the mean bed temperature for the cases selected that varies to a small extent only and approaches values of ~650.0 K. The mean temperature is determined by a global heat balance including net influx due to radiation and removal by convection of the primary air. Since these boundary conditions are constant, the mean temperature shows only small variations. The latter is caused by a different number of surface particles, that receive radiation, and therefore, determine the absolute value of total heat flux into the moving bed.

This characteristic is also reflected in the standard deviations shown in Figs. 15-17. Higher bar velocities cause an increased mixing rate that leads to a more homogeneous temperature distribution spanning a narrower range between minimum and maximum temperature. Thus a minimum deviation of ~100.0 K is achieved. A reduced deviation leads also to a more homogeneous reaction progress for a reacting packed bed, which favours an increased burn out for combustion or a more homogeneous product quality for processing.

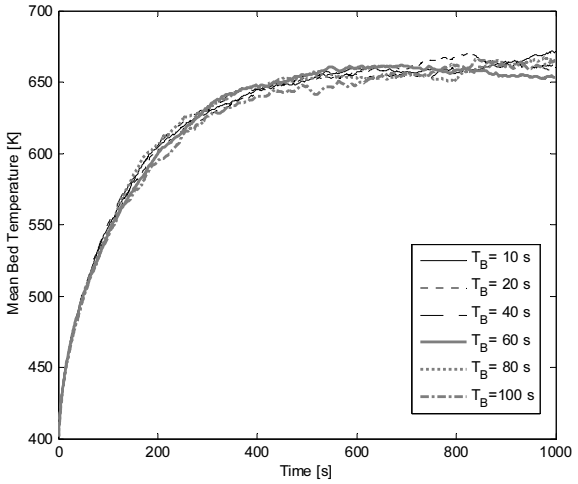

Fig. 12 Evolution of particles' mean temperature on a backward acting grate dependent on bar period and amplitude A_B = 0.062 m

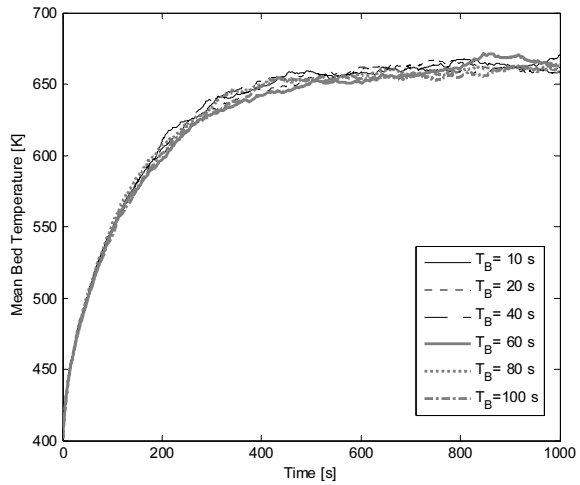

Fig. 13 Evolution of particles' mean temperature on a backward acting grate dependent on bar period and amplitude A_B = 0.124 m

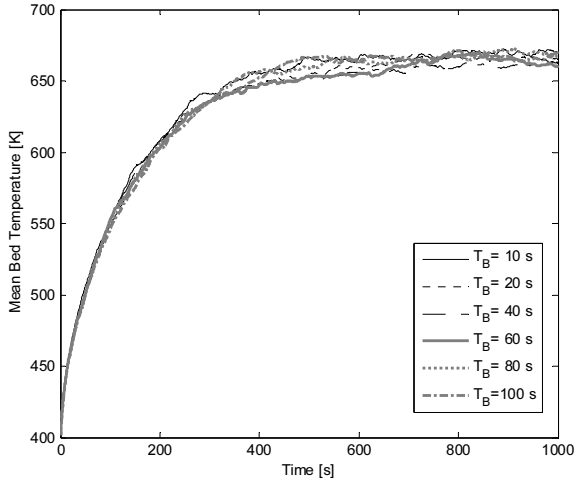

Fig. 14 Evolution of particles' mean temperature on a backward acting grate dependent on bar period and amplitude A_B = 0.186 m

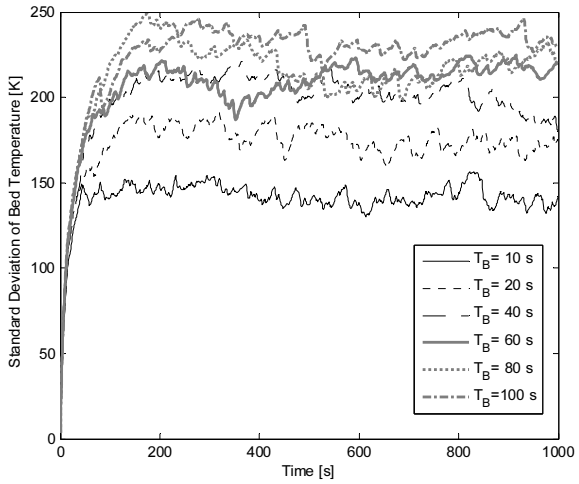

Fig. 15 Evolution of particles' standard deviation of temperature on a backward acting grate dependent on bar period and amplitude A_B = 0.062 m

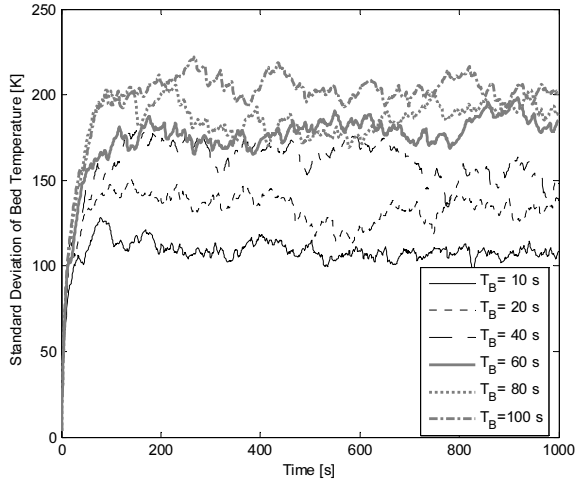

Fig. 16 Evolution of particles' standard deviation of temperature on a backward acting grate dependent on bar period and amplitude A_B = 0.124 m

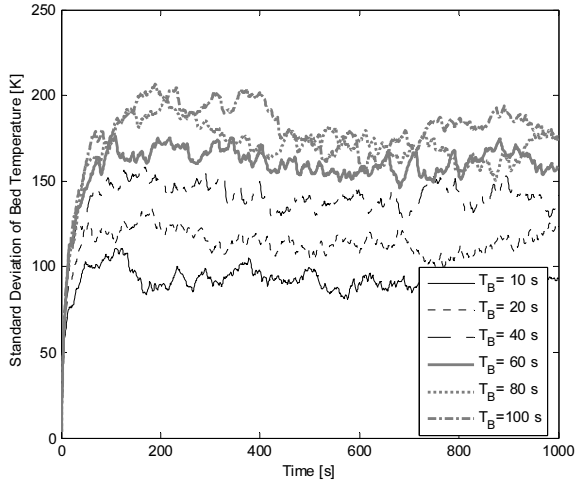

Fig. 17 Evolution of particles' standard deviation of temperature on a backward acting grate dependent on bar period and amplitude A_B = 0.186 m

The previously presented profiles for minimum, maximum and mean temperature including its standard deviation incorporate the bar velocity as a similarity parameter, and therefore, show a very homogeneous behaviour versus bar velocity in Fig. 18. Independent of the parameters amplitude and periodicity the profiles of minimum, maximum and mean temperature and deviation of Figs. 6 to 17 cumulate into one line for each parameter, clearly showing that the main parameter bar velocity determines the characteristics. The profiles indicate that an increased bar velocity causes a more homogeneous temperature distribution for the moving bed with a low standard deviation and a reduced difference between minimum and maximum temperature. Furthermore, the profiles in Fig. 18 tend to approach almost finite values for higher bar velocities larger than 0.03 m/s. It indicates that an increase of bar velocities does not necessarily lead to a more homogeneous temperature distribution.

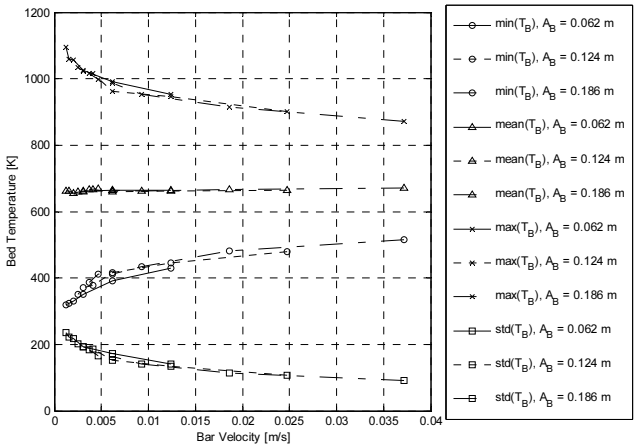

Fig. 18 Steady state minimum, maximum, mean temperatures including its standard deviation on a backward acting grate versus bar velocity

3.2. Classification of particle temperatures

The statistical analysis carried out yielded already important quantities of the heat-up process of a moving bed on a backward acting grate. However, important parameters vanish due to statistical averaging, in particular characteristics such as temperatures of individual particles. In order to retrieve more details of the temperature distribution, temperatures of the particles were classified versus time depicted in Fig. 19 for an amplitude of $A_B = 0.124$ m and a periodicity of $T_B = 20$ s.

Temperature classes were chosen with a width of 100 K between a minimum temperature of 300 K and a maximum temperature of 1100 K. The labels of the temperature classes represent always the mean temperature of a class meaning the respective class extends by a value of ± 50 K around this value. Hereafter, the number of particles falling into the temperature classes were determined at each time step yielding a distribution versus time and temperature classes as depicted in Fig. 19.

Since all particle temperatures were initialised uniformly, all particles appear initially in one temperature class. Hereafter, individual temperatures develop, that redistributes them into different temperature classes. Towards the end of the simulation period after ~600 s a clear peak develops at a temperature of ~550 K with a decreasing profile to higher and lower temperature classes. Furthermore, the classification in Fig. 19 approaches an almost steady state behaviour at the end of the simulation period. Thus, time-averaging of classification profiles for all cases considered was carried out and are arranged in a three-dimensional plot versus bar mean velocity shown in Fig. 20.

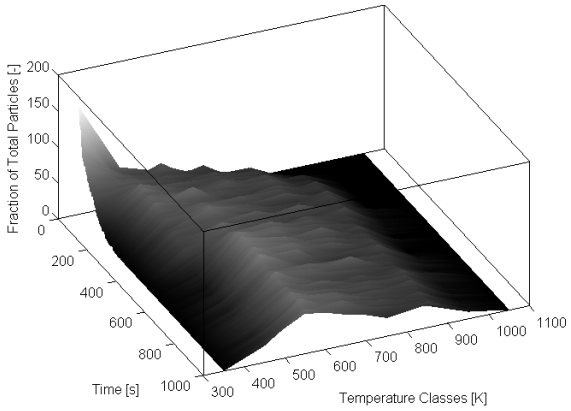

Fig. 19 Classification of particle temperatures versus time for a backward acting grate subject to a bar amplitude of $A_B = 0.124$ m and a periodicity of $T_B = 20$ s

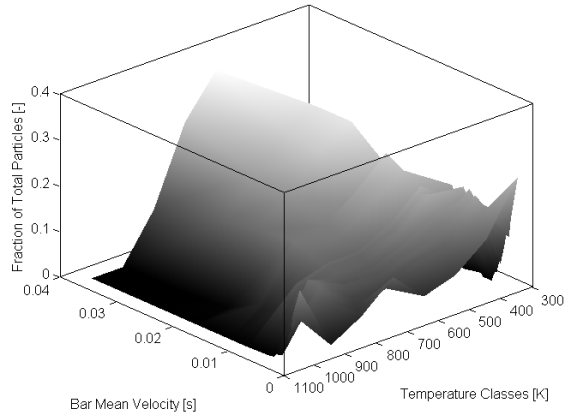

Fig. 20 Time-averaged clasification of mean temperatures on a backward acting grate versus bar velocity

The profile is very distinguished for bar velocities higher than ~0.02 m/s and does not show further variations. Hence, the population of temperature classes is independent of bar velocity for the operation range investigated. However, a distribution with rather large fluctuations is encountered for lower bar velocities, that does not indicate common characteristics.

4. Conclusions

The heat-up process of a moving bed of fir wood particles on a backward acting grate was investigated by the DPM. The latter predicts the spatial and temporal varying temperature distribution for each particle of the packed bed by solving the transient and one-dimensional differential conservation equation for energy. Particles of spherical shape were arranged on a backward acting grate and a constant radiative flux was employed onto the surface of the bed. The radiative surface flux reaches only particles on the surface of the packed bed, which transferred heat into the interior of the packed bed by conduction and radiation between neighbouring particles. Statistical parameters such

as minimum and maximum temperature in conjunction with a mean bed temperature and its standard deviation were estimated for different amplitudes and periodicities of the grate bars. Results show that:

1. The bar velocity is the sole influencing parameter as compared to amplitude and periodicity.

2. High bar velocities force a more homogeneous temperature distribution within the moving bed with reduced standard deviation. Consequently, maximum temperatures decrease with higher bar velocity, whereas minimum temperatures increase.

Acknowledgements

This research was funded by grant (No. ATE-02/2012) from the Research Council of Lithuania.

References

1. **Smirnov, E.I.; Muzykantov, A.V.; Kuzmin, V.A.; Kronberg, A.E.; Zolotarskii, I.A.** 2003. Radial heat transfer in packed beds of spheres, cylinders and raschig rings: Verification of model with a linear variation of λ_{er} in the vicinity of the wall, Chemical Engineering Journal 91: 243-248. http://dx.doi.org/10.1016/S1385-8947(02)00160-2.
2. **Smirnov, E.I.; Kuzmin, V.A.; Zolotarskii, I.A.** 2004. Radial thermal conductivity in cylindrical beds packed by shaped particles, Chemical Engineering Research and Design 82(A2): 293-296. http://dx.doi.org/10.1205/026387604772992891.
3. **Figueroa, I.; Vargas, W.L.; McCarthy, J.J.** 2010. Mixing and heat conduction in rotating tumblers, Chemical Engineering Science 65: 1045-1054. http://dx.doi.org/10.1016/j.ces.2009.09.058.
4. **Laguerre, O.; Amara, S.B.; Alvarez, G.; Flick, D.** 2008. Transient heat transfer by free convection in a packed bed of spheres: Comparison between two modelling approaches and experimental results, Applied Thermal Engineering 28: 14-24. http://dx.doi.org/10.1016/j.applthermaleng.2007.03.014
5. **Laguerre, O.; Amara, S.B.; Flick, D.** 2006. Heat transfer between wall and packed bed crossed by low velocity airflow, Applied Thermal Engineering, 26: 1951-1960. http://dx.doi.org/10.1016/j.applthermaleng.2006.01.011
6. **Swailes, D.C.; Potts, I.** 2006. Transient heat transport in gas flow through granular porous media, Transp. Porous Media 65: 133-157. http://dx.doi.org/ 10.1007/s11242-005-6090-7.
7. **Venugopal, G.; Balaji, C.; Venkateshan, S. P.** 2010. Experimental study of mixed convection heat transfer in a vertical duct filled with metallic porous structures, International Journal Thermal Science 49: 340-348. http://dx.doi.org/10.1016/j.ijthermalsci.2009.07.018.
8. **Thoméo, J.C.; Grace, J.R.** 2004. Heat transfer in packed beds: experimental evaluation of one-phase water flow, Braz. J. Chem. Eng. 21(1). http://dx.doi.org/10.1590/S0104-66322004000100003.
9. **Fanaei, M.A.; Vaziri, B.M.** 2009. Modeling of temperature gradients in packed-bed solid-state bioreactors, Chemical Engineering and Processing 48: 446-451. http://dx.doi.org/10.1016/j.cep.2008.06.001.
10. **Moreira, M.F.P.; Ferreira, M.C.; Freire, J.T.** 2006. Evaluation of pseudohomogeneous models for heat transfer in packed beds with gas flow and gas-liquid cocurrent downflow and upflow, Chemical Engineering Science 61: 2056-2068. http://dx.doi.org/10.1016/j.ces.2005.11.003.
11. **Regin, A.F.; Solanki, S.C.; Saini, J.S.** 2009. An analysis of a packed bed latent heat thermal energy storage system using pcm capsules: Numerical investigation, Renewable Energy 34: 1765-1773. http://dx.doi.org/10.1016/j.renene.2008.12.012.
12. **Ulson de Souza, S.M.A.G.; Whitaker, S.** 2003. Mass transfer in porous media with heterogeneous chemical reaction, Braz. J. Chem. Eng. 20(2): 191-199. http://dx.doi.org/10.1590/S0104-66322003000200013.
13. **Polesek-Karczewska, S.** 2003. Effective thermal conductivity of packed beds of spheres in transient heat transfer, Heat and Mass Transfer 39: 375-380. http://dx.doi.org/10.1007/s00231-002-0343-6.
14. **MacPhee, D.; Dincer, I.** 2009. Thermal modeling of a packed bed thermal energy storage system during charging, Applied Thermal Engineering 29: 695-705. http://dx.doi.org/10.1016/j.applthermaleng.2008.03.041
15. **Lee, J.-J.; Park, G.-C.; Kim, K.-Y.; Lee, W.-J.** 2007. Numerical treatment of pebble contact in the flow and heat transfer analysis of a pebble bed reactor core, Nuclear Engineering and Design 237: 2183-2196. http://dx.doi.org/10.1016/j.nucengdes.2007.03.046
16. **Mei, H.; Li, C.; Liu, H.** 2005. Simulation of heat transfer and hydrodynamics for metal structured packed bed, Catalysis Today 105: 689-696. http://dx.doi.org/10.1016/j.cattod.2005.06.042.
17. **Yang, J.; Wang, Q.; Zeng, M.; Nakayama, A.** 2010. Computational study of forced convective heat transfer in structured packed beds with spherical or ellipsoidal particles, Chemical Engineering Science 65: 726-738. http://dx.doi.org/10.1016/j.ces.2009.09.026.
18. **Augier, F.; Idoux, F.; Delenne, J. Y.** 2010. Numerical simulations of transfer and transport properties inside packed beds of spherical particles, Chemical Engineering Science 65: 1055-1064. http://dx.doi.org/10.1016/j.ces.2009.09.059.
19. **Papadikis, K.; Gu, S.; Bridgewater, A.V.** 2010. Computational modelling of the impact of particle size to the heat transfer coefficient between biomass particles and a fluidised bed, Fuel Processing Technology 91: 68-79. http://dx.doi.org/10.1016/j.fuproc.2009.08.016.
20. **Nithiarasu, P.; Seetharamu, K.N.; Sundararajan, T.** 2002. Finite element modelling of flow, heat and mass transfer in fluid saturated porous media, Arch. Computational Methods in Engineering 9(1): 3-42. http://dx.doi.org/10.1007/BF02736231.
21. **Peters, B.; Džiugys, A.; Navakas R.** 2011. Simulation of thermal conversion of solid fuel by the discrete particle method, Lith. J. Phys. 51(2): 91-105. http://dx.doi.org/10.3952/lithjphys.51204.
22. **Gronli, M.** 1996. A theoretical and experimental study of the thermal degradation of biomass, PhD thesis, The Norwegian University of Science and Technology Trondheim.
23. **Kaume, M.** 2003. Transportvorgänge in der Verfahrenstechnik. Springer. http://dx.doi.org/10.1002/cite.200590014.
24. **Hänel, D.** 2004. Molekulare Gasdynamik, Springer.

25. **Peters, B.** 2003. Thermal Conversion of Solid Fuels, WIT Press, Southampton.
26. **Peters, B.; Džiugys, A.; Hunsinger, H.; Krebs, L.** 2005. An approach to qualify the intensity of mixing on a forward acting grate, Chem. Eng. Sci. 60(6): 1649-1659. http://dx.doi.org/10.1016/j.ces.2004.11.004.

B. Peters, A. Džiugys

ŠILUMOS MAINŲ ANT ATBULINĖS EIGOS ARDYNO ĮVERTINIMAS

R e z i u m ė

Straipsnyje nagrinėjamas ardyno laiptelio judėjimo poveikis dalelių įkrovos, esančios ant atgalinio ardyno, įšilimui. Šilumos mainai judančių dalelių įkrovos viduje nemažai lemia atskirų dalelių temperatūras, o kartu ir chemines reakcijas, vykstančias įkrovos dalelėse. Taigi išsamesnės žinios apie šilumos mainus įkrovoje leidžia geriau įvertinti reakcijos eigą. Dalelių judėjimas ir šilumos mainai ant atgalinio ardyno išreiškiami naudojant diskrečiųjų dalelių modelį. Skirtingai nuo ištisinės terpės aprašymo, šiuo atveju įkrova laikoma susidedančia iš baigtinio skaičiaus atskirų dalelių. Dalelių judėjimas išreiškiamas taikant diskrečiųjų elementų metodą (DEM), o dalelių temperatūros nustatomos sprendžiant energijos tvermės lygtis. Dalelės kaitinamos spinduliuote, veikiančia įkrovos paviršių, o šilumos mainai vyksta tarp artimų dalelių šiluminio laidumo ir tarpusavio spinduliuotės. Taip pat atsižvelgiama į papildomus šilumos mainus su aplinkine dujine terpe dėl konvekcijos.

B. Peters, A. Džiugys

EVALUATION OF HEAT TRANSFER ON A BACKWARD ACTING GRATE

S u m m a r y

Within this contribution the effect of the kinetics of bar motion on the heat-up characteristics of a packed bed, consisting of biomass or municipal waste, on a backward acting grate is investigated. Transfer of heat within a packed bed of moving particles determines to a large extent the individual temperatures of particles, and therefore, any reaction process attached to the particles e.g. packed bed. Thus, a deeper knowledge of heat transfer in a packed bed allows for a better assessment of the reaction progress. Both motion and heat-up of particles on a backward acting grate are predicted by the Discrete Particle Method (DPM). Contrary to continuum mechanic approaches, a packed bed consists of a finite number of individual particles. Motion of particles is predicted by the Discrete Element Method (DEM), whereas the particles' temperatures are determined by the solution of the conservation equation for energy. Particles are heated by a radiative flux on the surface of the packed bed and exchange heat by conduction and radiation with particles in their proximity. Additional heat transfer to the surrounding gas phase by convection is also taken into account.

Keywords: Waste management technologies, Discrete Particle Method, Discrete Element Method, heat-up, backward acting grate.

Received March 14, 2013
Accepted January 21, 2014